

# Spike Synchronization Dynamics of Small-World Networks

Derek Harter  
Texas A&M University - Commerce  
Commerce, TX USA  
Derek.Harter@tamuc.edu

November 6, 2021

## Abstract

In this research report, we examine the effects of small-world network organization on spike synchronization dynamics in networks of Izhikevich spiking units. We interpolate network organizations from regular ring lattices, through the small-world region, to random networks, and measure global spike synchronization dynamics. We examine how average path length and clustering effect the dynamics of global and neighborhood clique spike organization and propagation. We show that the emergence of global synchronization undergoes a phase transition in the small-world region, between the clustering and path length phase transitions that are known to exist. We add additional realistic constraints on the dynamics by introducing propagation delays of spiking signals proportional to wiring length. The addition of delays interferes with the ability of random networks to sustain global synchronization, in relation to the breakdown of clustering in the networks. The addition of delays further enhances the finding that small-world organization is beneficial for balancing neighborhood synchronized waves of organization with global synchronization dynamics.

*Keywords:* small-world, spiking dynamics, network graph analysis, synchronization

# 1 Introduction

## 1.1 Neural Oscillations and Neural Constraints

The emergence of global synchronized behavior in biological brain neural oscillations may be important for many types of information processing tasks. Global synchronized waves are thought to play roles in multi-sensory feature binding, global information transfer, consciousness and rhythmic motor entrainment, among other functions [5, 13]. In this work we investigate the effects that global network architecture have on micro and macro synchronization of spiking neuronal units. The roles or usefulness of synchronization are not the subject of this paper, but simply what types of synchronization dynamics are facilitated or suppressed as network architectures vary in their properties of how far and how long information must travel in the network to get to its destination, and how cohesive neuronal groups are in the information processing network.

Some basic features of brain networks appear to be highly conserved over different scales and types of measurement [3, 2]. The archetypal brain network appears to be a small-world network, with relatively short path lengths for information to travel along and with high local neighborhood clustering. The former logically affects the efficiency of global information processing, while clustering is useful in robustness and error tolerance. Brain networks appear to have scale-free degree distributions, where a few hub nodes have large numbers of connections while the majority of neural units have small numbers of connections, both of which are compatible with clustering and highly modular hierarchical neighborhood organization. Brain networks and nervous systems are highly constrained by the world they must operate within. Brain networks have neither unlimited space nor energy in order to perform their crucial information processing functions. Brain networks must accomplish their tasks adequately while conserving material and providing adequate energy for the system. Anatomical networks are sparsely connected and wiring lengths are close to minimal, which certainly reflects the physical and energy constraints that the brain faces in order to function.

The structure and reflected function of brain networks, seen on many different scales, may be the result of the evolution and development of the systems under these constraints. Brain networks are spatially embedded, with physical constraints, and rely on biological processes to keep them supplied with energy. Brains must achieve highly efficient information processing



and information transfer while maintaining low connection and energy costs. As Bullmore and Sporns state [3, p. 196]:

If wiring cost was exclusively prioritized the network would be close to a regular lattice, whereas if efficiency was the only selection criterion the network would be random. The existence of a few long-range anatomical connections can deliver benefits in terms of efficiency and could arguably account for the evolution of economical small-world properties in brain networks at all scales.

The functional behavior of networks with small-world and scale free structures have, of course, been studied in the past. In [4] the authors develop a hierarchical organization of sparsely connected internal neurons that form domains (or clusters). The clusters were organized into a type of echo state network (ESN), but instead of being a random network as in a typical ESN, they subjected the ESN reservoir to incremental growth rules in order for form a scale-free degree distribution of the reservoir clusters. They mainly applied their architecture to solving prediction problems. The system, in theory with its organization, can be scaled to reflect some of the same natural characteristic of scale-free biological neural networks, such as fast signal propagation and coherent synchronization. In [12], the work most similar to the present research, the authors investigated synchronization in small-world networks as well. In this paper, the authors showed with some analytic results as well as simulations, that with sufficient weights and large enough networks, that a small-world network of continuous-time oscillators will synchronize, even if the original nearest-neighbor coupled networks cannot achieve synchronization under the same conditions. The present research supports these basic findings, as we also show empirically for spiking networks that global synchronization is possible with sparsely connected networks with a few long-range interconnections (small-world), but impossible for regular networks.

In this research, we investigate some of the questions raised in this view of brain networks as systems that have evolved under energy and spatial constraints in order to optimize information processing. Brain networks are especially good at being both flexible and inventive, but robust both in the face of uncertainty and also in the face of structural damage or other difficulties. Better understanding how and why small-world organization under such constraints evolve and how they support robust information processing is the goal of research such as that presented in this report.

## 1.2 Small-world Networks

We have mentioned small-world network organization previously, and the concept plays an important part in this presented research report. In this section we will review the Watts and Strogatz (WS) interpolation model, and explain some of the basic features of small-world network organization. The idea of small-world organization had been around for some time before the WS model formalized the concept. Stanley Milgram [11] showed empirically the possible existence of small-world organization in human social networks in 1967 by mailing letters to random people, asking them to send to someone they know, who would in turn forward to someone they know, with the goal of returning it back to the sender. The chain such letters took showed a surprisingly short number of connections needed on average to connect any two people (the so called six-degrees of separation concept).

In 1998, WS proposed their interpolation model that demonstrated the concept of small-world networks [14] by creating networks that are intermediate between a regular (ring) lattice and a random graph. A ring lattice is simply a network of nodes organized in a circle, where each node is connected to  $k$  of its nearest neighbors. A random network, as the name implies, is a set of nodes whose connections have been generated randomly, in the general case where each connection has an equal probability  $p$  of existing (see Figure 1). Random networks were first explored by Erdős and Rényi [6], and the general class of models are known as Erdős-Rényi (ER) random graphs.

Small-world networks are networks that show both a relatively low average path length, but at the same time exhibit high degrees of local clustering. Here average path length is easy to understand, the minimal path length between any two nodes is the smallest distance (in a weighted graph) or number of hops (in an unweighted graph) that you need to travel to get from any particular starting point to any particular destination. The average path length (called simply  $L$ ) is then simply the average of all the minimal path lengths between all possible pairs of nodes. Clustering ( $C$ ) is also a fairly simple measure of a network, it measures to what degree nodes are connected to one another. For example, to calculate  $C$ , take all of the immediate neighbors of a node. For this set of nodes, determine the number of possible connections between all the nodes, and the number of actual connections that exist in the graph. The ratio of the actual to the possible connections in the neighborhood is the clustering coefficient for the original node. The average clustering  $C$  over the graph is simply the average clustering coeffi-

cient calculated over all nodes. See [3] for a good review of these and other network graph properties.

For a completely regular network, like a ring lattice where  $N$  nodes are organized in a circle, and each node is connected with its  $k$  nearest neighbors along the ring,  $C$  is very high, because neighbors of any node tend to be connected with one another. However, in a regular ring lattice, the average path lengths are relatively long, because there are no long-range connections, and thus you are forced to take many small hops to get from one side of the ring to the other. For a random network, however, the properties of  $C$  and  $L$  are reversed. In a random network, average path lengths are short, because of the nature of the random connectivity. However, there is no real clustering to speak of, as the neighbors of any node are unlikely to be connected to one another. WS showed that, as we move from a regular ring lattice towards a random network there is a region of the networks that display both a beneficial low  $L$  while still retaining high  $C$ . They also showed that both  $L$  and  $C$  perform a rapid transition when interpolating from regular to random networks, but these phase transition occurs at different locations in the phase space. This region of low path lengths but high neighborhood clustering is known as the small-world region (see figure 4).

### 1.3 Izhikevich Spiking Networks

Using the Watts and Strogatz interpolation algorithm, we will be generating networks that vary from regular through small-world to random networks. However, in this research report, we are interested in studying the functional dynamics that such networks might support. We will be using standard Izhikevich spiking units for this purpose [9]. Izhikevich introduced a model of spiking units that were both computationally efficient and easy to simulate, as well as capable of producing rich firing dynamics seen in real biological neurons [10]. The Izhikevich spiking model has become very popular because of these reasons for simulating spiking network dynamics. In the original 2003 paper, Izhikevich showed an example of synchronized behavior in a network of  $N = 1000$  Izhikevich units. In this example, the network was fully connected (every unit had a connection to every other unit). He also had a mix of excitatory and inhibitory units (in a ratio of 800 excitatory to 200 inhibitory units). The model defines only two variables to describe a neural unit: the voltage, or membrane potential of a neuron  $v$ , and a membrane recovery variable  $u$ , with an auxiliary after-spike reset defining a

spike as occurring when the membrane potential reaches or exceeds  $30mV$ . A number of parameters may be set in the model in order to produce the rich set of spiking pattern dynamics mentioned.

All networks presented in this research report use Izhikevich spiking units with network size  $N = 1000$  and a ratio of excitatory to inhibitory units of  $N_e = 800$ ,  $N_i = 200$ . However our networks are sparsely connected. Our units will be layed out on a ring lattice, with connectivity  $k = 10$  connecting each unit to its 10 closest neighbors (5 clockwise and 5 counterclockwise). Therefore our networks have  $10^4$  connections out of a possible  $\approx 10^6$  connections (1% of the potential connections). As we discussed earlier, this sparseness is more indicitative of biological networks. Laying out the units in a ring also serves several purposes. It embeds the network in a spatial context, thus giving a meaning to the distance between nodes, and the length of connections between nodes. These wiring lengths will be used in the second simulation to provide a proportional propagation delay to the signals transmitted as spikes along the network connections.

## 1.4 Research Questions

In the work presented here, our main research question is: how are local and global synchronization of unit spiking effected by network architecture? In particular, does synchronization across a large network of spiking units appear to be related to the path lengths available for the transmission of information across the network? Also, how does clustering, or the cliquishness of neighbors, affect spiking dynamics? In this work, we assume that global synchronization of spiking behavior is in some sense good, and is necessary for such crucial tasks in biological brains such as multi-modal integration, attentional focus and awareness, conscious processing, etc. In the models presented in this paper, we therefore make a simplifying assumption that the ability to form network wide synchronized spiking behavior indicates a positive capability of the network, and when such global behavior is not possible, the networks are deficient in their ability to perform global information processing tasks.

In the following simulations, we use the WS interpolation method in order to vary network architecture from a completely regular (ring) lattice, through the small-world region up to a completely random graph. We will use the WS interpolation method to form networks of Izhikevich spiking units [9], connected with the varying properties of  $L$  and  $C$  as we simulate

networks transitioning through this parameter space. We show that spiking synchronization dynamics are highly dependent on  $L$  and  $C$  parameters, and have a phase transition in the same small-world region from an inability to form global synchronization, to a strong ability to form global synchronized behavior.

We further investigate in these simulations, the question of what role wiring length or cost may play in the formation of global synchronized behavior. In particular, we investigate the cost of wiring length in the form of a more realistic propagation delay of spiking signal information. Most simulations of spiking networks are performed without taking into account the real cost of wiring or path length in terms of the dynamical behavior. In this paper, we show that wiring length, in the form of such propagation delays, does interfere with the ability of a network to form global synchronization, as one would expect. Thus global synchronization may also be constrained by the average path length  $L$  needed to propagate information, which gives another reason why completely random networks may be worse, in an information processing sense, than networks in the small-world region for doing information processing tasks that require global or at least more large-scale regional synchronization in order to properly function.

In the following sections, we will first present our general methods and models used in the simulations in this paper. We will next discuss the specifics of two experiments, illustrating the effects of small-world network architecture on global spiking synchronization behavior, both without and with propagation delay of spike firings. We conclude with a more general discussion of the simulation results, and conclusions and ideas for future investigations.

## 2 Method

### 2.1 Izhikevich Spiking Network Model

In all of the simulations<sup>1</sup> presented in this work, we use standard Izhikevich units, as first described in [9]. In that original work, a spiking model was presented that is both computationally efficient, but capable of displaying a large range of spiking dynamics similar to those seen in real biological spiking

---

<sup>1</sup>All simulations, scripts and data analysis artifacts used in this research report can be found at and reproduced from <https://bitbucket.org/dharter/sync-dyn-small-world-net>.

networks. Izhikevich units define only two variables to simulate the activity of a unit, the membrane potential  $v$  and a membrane recover variable  $u$ , with an auxiliary after-spike resetting rule:

$$v' = 0.04v^2 + 5v + 140 - u + I \quad (1)$$

$$u' = a(bv - u) \quad (2)$$

$$\text{if } v \geq 30\text{mV, then } \begin{cases} v \leftarrow c \\ u \leftarrow u + d \end{cases} \quad (3)$$

The  $a, b, c, d$  parameters can be set to produce different spiking dynamics.  $I$  represents input to the unit, which comes from a combination of randomly generated thalamic background input, plus input received from connected units generated from their spike firings. We used two sets of these parameters, one for excitatory units and one for inhibitory units, the same as in the original Izhikevich example.

In the [9] model description, Izhikevich showed an example of synchronized spiking behavior in a fully connected network of  $N = 1000$  units. Our simulations also use  $N = 1000$ , but in sparsely connected networks with varying properties connected as ring lattices (see next section). We also use the same mix of two types of basic units, excitatory ( $N_e = 800$ ) and inhibitory ( $N_i = 200$ ). Excitatory and inhibitory weights, as well as simulated random thalamic input, were chosen in order to best illustrate the changing spiking synchronization dynamics. However, it appears that the dynamics reported in this research are robust over a wide range of parameters in the weight and thalamic stimulation space. All weights and external thalamic input parameters are generated randomly, using a uniform distribution on the open interval  $[0.0, 1.0)$ , multiplied by the indicated parameter value. Table 1 gives a summary of all of the important parameters, and their settings used in all Izhikevich spiking networks presented in this research.

## 2.2 Small-World Interpolation

We organized the spiking networks as ring lattices, both to give a meaning of spatial layout and distance associated with wiring lengths, as well as to reproduce the WS interpolation from regular to random networks (see Figure 1). All simulations in this paper consisted of an initial ring lattice of  $N =$

Table 1: Parameters used for all Izhikevich network simulations.

Parameter	Description	Value
$N$	Total units in simulation network	1000
$N_e$	Number of excitation units in network	800
$N_i$	Number of inhibitory units	200
$w_e$	The excitatory weight scaling factor	32
$w_i$	The inhibitory weight scaling factor	22
$t_e$	The amount of random thalamic stimulation for excitatory units	3
$t_i$	The amount of random thalamic stimulation for inhibitory units	11

1000 units. All units were connected to their  $k = 10$  nearest neighbors, as in the original Watts and Strogatz analysis. Here nearest neighbor is defined spatially along the ring, so for  $k = 10$  connectivity, the 5 closest neighbors clockwise and counterclockwise were connected. In terms of the propagation of spikes, the generated networks were treated as directed networks, so while initially neighbors would be connected with one another, the weight of the connections can be different from source to destination unit and back from destination to source. Likewise, random rewiring only affected one directed connection at a time, so two units connected to one another might not be reciprocally connected after random rewiring. All networks thus had 10,000 total connections in the network (  $k = 10 \times N = 1000$  ). Also note that this means that only a total of 1% of the possible connections are present when compared to a fully connected network (  $10^4$  actual connections of  $10^6$  potential connections).

Interpolation from regular lattice to random network was recreated as described in [14]. The basic algorithm is as follows:

1. Create a regular ring lattice of size  $N$  nodes and connectivity  $k$ .
2. Examine every (directed) edge. With probability  $p$  reconnect the edge to a new randomly selected destination. The destination is selected among all nodes (except the source) with uniform probability.

When  $p = 0$ , no rewiring occurs, and we end up with the same regular ring lattice we started with (Figure 1, left). When  $p = 1.0$ , every connection

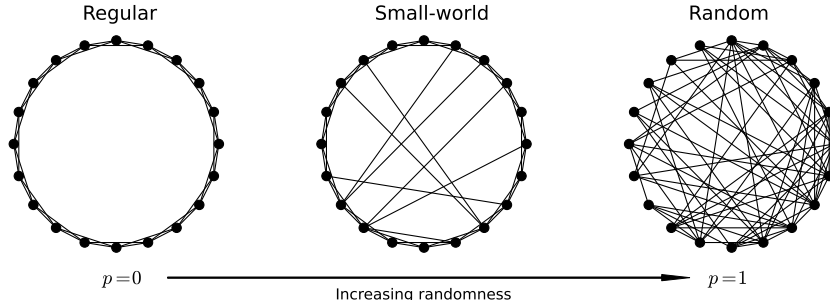


Figure 1: WS interpolated network results. The example ring lattices shown here have  $N = 20$  units and  $k = 4$  connectivity.  $p$  is the probability of rewiring a connection during interpolation.

is rewired and the result is a randomly connected network (Figure 1, right). As  $p$  increases, at first a small number of long-range interconnects are formed (Figure 1, middle). This is the beginning of the small-world region of network organization. As  $p$  increases from  $0.0 \rightarrow 1.0$ , the network experiences phase changes at different locations of  $p$  for crucial measurements such as  $C$  and  $L$ . Further there are large areas where clustering  $C$  is high, as in a regular lattice, but  $L$  is low, indicating short average path lengths for global communication. This area of network connectivity with high  $C$  but low  $L$  is known as the small-world region (see figure 4).

### 2.3 General Network Spiking Dynamics

Figure 2 shows a typical example of network activity obtained with networks structured as described previously. This figure was produced with  $p = 0.001$ , so within the small-world region, but still fairly regular with relatively large average path lengths  $L$ . In this figure, we show a standard raster plot of spike firings at the bottom, and a summary of spike counts in the middle part of the figure. Both plots show activity for  $2000ms$  of simulated time. Raster plots are simply obtained by plotting a point for every unit, at every time step where the unit is considered to have fired a spike. For Izhikevich units, this is when  $v > 30$ , e.g. when the unit voltage exceeds its spike reset threshold. The middle part of Figure 2 shows a crude measure of overall network activity. This measure is obtained simply by counting up all of the spikes that occur at each discrete simulated time step.



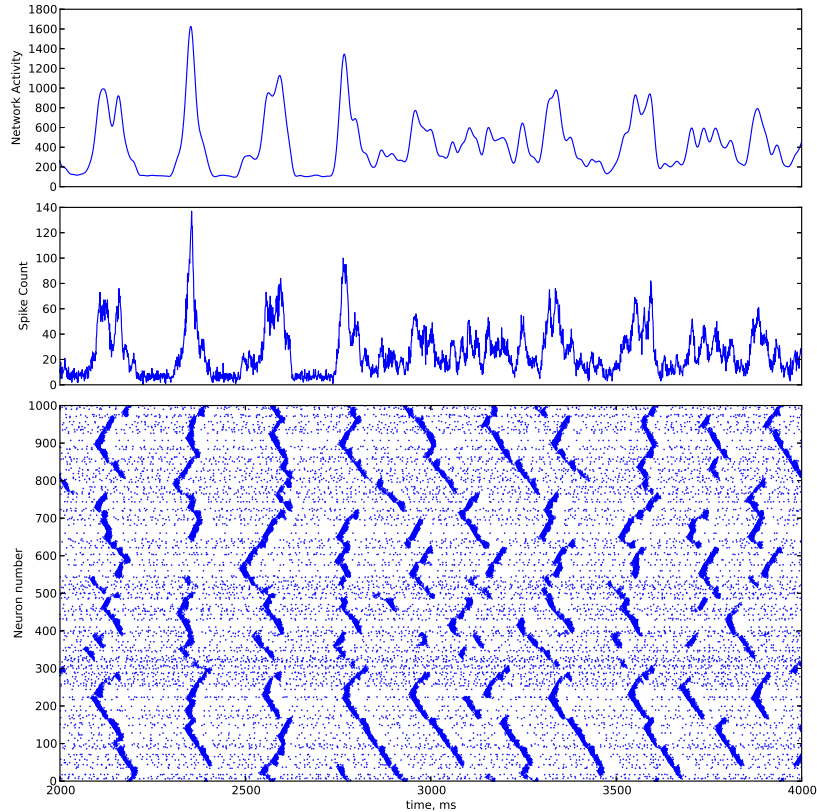


Figure 2: Spike (scatter) plot (bottom), simple count of spikes at each time step (middle), and convoluted summary of overall mean field spiking activity (top).

Overall this figure demonstrates a few properties of the spiking dynamics of our ring based regular lattices composed of Izhikevich spiking units. For completely regular lattices, at the weights and thalamic stimulation we are using, highly clustered  $C$  networks show a tendency to produce ripples or waves of spikes that travel from initiator spots around the ring. Overall coherence and synchronization is not possible for  $p = 0$  and low  $p$  networks, because spike waves must travel in many hops to propagate around the ring. The overall measure of network activity shows some oscillations, but clearly indicates a lack of organized global structure. As  $p$  increases, however, global synchronization is enhanced, as we will see when interpolate the networks through the range of  $p$  values.

## 2.4 Enhancing Detection of Synchronized Behavior

We found that a simple count of spike activity was a poor measure of global network synchronization for a couple of reasons. When used to estimate the frequency and power of coherent network wide synchronized waves, simple spike activity hides much of the co-activation information present. Spikes that occur within a few, or even just 1, ms apart do not contribute to a measure of synchronization.

We enhanced the detection of synchronized firings by convolving each spike train with a convolution kernel:

$$y = e^{-\left(\frac{x}{10}\right)^2} \quad (4)$$

We used a window width of  $30ms$  for our convolution function. This has the effect, when summing up spiking behavior, to allow spikes within a  $\pm 15ms$  window to contribute at least some to the measure of synchronous firing. Of course, because of the function we convolved the spikes with, signals  $15ms$  apart contribute much less to each other than when firing at the same time, but still in general this helps to detect overall synchronized activity, even if it is spread over a window. In our tests, the size of the window did not significantly alter the results we report, with convolution windows from as small as 6 to as large as 200. After convolving all spike trains, we sum up the convolved activity of all units to get a measure of network activity over time. Figure 2 top, from the previous section, displays the overall network activity measured using the convolved kernel window. As you can observe, the effect is to significantly smooth the activity, which also helps in analyzing frequency components. This is effectively calculating the local field potential of the simulated network.

In this research, we introduce a measure of global synchronized network behavior called  $S$ , based on the overall convolved spiking activity. We define  $S$  as the power of the dominant frequency of the convolved network activity.  $S$  is obtained through a standard power spectrum analysis, using the fast Fourier transform, from which we determine the frequency at which the maximum power component was present in the signal. For Figure 2, we obtained a  $S = 3.5e^{11}$  power signal at a frequency of  $6.8Hz$ .

## 3 Experiments

### 3.1 Simulation 1: Network Synchronization Dynamics

In simulation 1, we will look at how spike synchronization dynamics are affected as  $p$ , the probability of rewiring, is interpolated through the small-world region, from completely regular to completely random networks. We explore the space of  $p$  values so that we can see how behavior changes as a function of  $p$ . For each  $p$ , we run  $NUM\_SIMS = 100$  simulations and report the average value of the measured properties.

First we look at typical spiking and network activity in three regions of the  $p$  space for our simulations. In Figure 3, we show spiking and network activity of 3 separate networks,  $p = 0.0, p = 0.02, p = 1.0$ . As in the previous figures, the top part of the figure shows the overall convolved network activity, or local field potential of the network, while the bottom shows a spike raster plot of all of the spiking activity of all of the units for the selected time period. Regular lattice dynamics are typically realized as waves of activity propagating around the ring, as seen in the figure, left. Since long range connections are not present, by necessity information such as a wave of spikes must propagate from unit to unit, cluster to cluster. As we increase  $p$ , more and more long range connections are formed, shortening overall path lengths. The middle portion of Figure 3 shows activity for a network firmly within the small-world region of the  $p$  parameter space. With only 2% of connections rewired, we see significantly more ability for spikes to synchronize globally. Here, already, looking at the global network activity it is easy to identify global synchronized spike waves, occurring at a regular frequency. On the right side of Figure 3 we show activity of the random network, where  $p = 1.0$ . Random networks are characterized by connections that jump across the ring, so synchronized activity is easily and readily achievable. Here all units regularly fire in bursts within very small windows. Frequencies achieved for global synchronization range from about  $9Hz$  to  $15Hz$  typically. The characteristic frequency appears to be a function of the network size for our simulations.

In order to measure overall synchronization, we ran simulations across the spectrum of  $p$  rewiring probabilities and measured the previously defined network synchronization parameter  $S$ . We ran  $NUM\_SIMS = 100$  simulations for each  $p$  value and averaged the result of all simulations for the same  $p$ . The results of this set of simulations is presented in Figure 4. In this figure

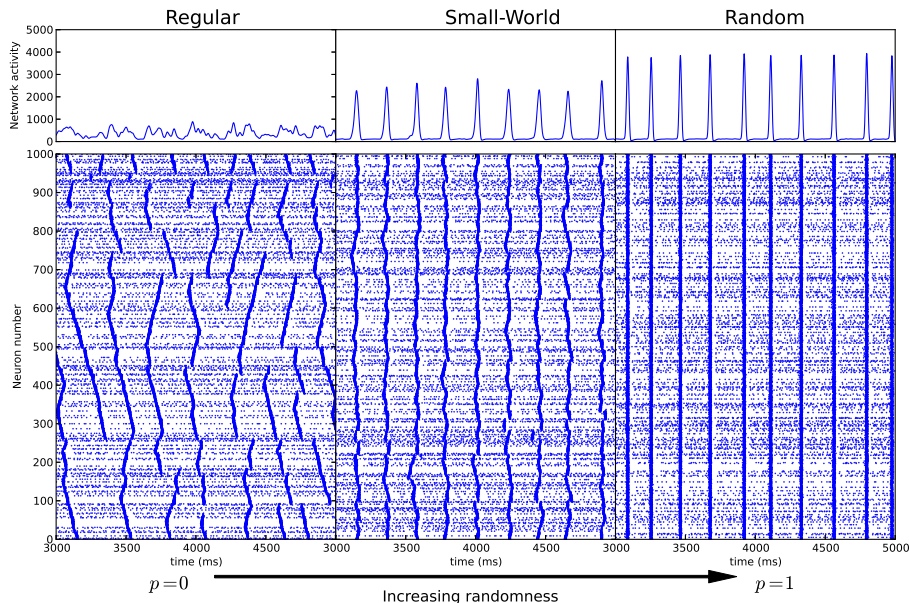


Figure 3: Typical network/unit dynamics of simulation 1. Left,  $p = 0$  regular lattice. Middle,  $p = 0.02$  small-world. Right,  $p = 1$  random network. Top, convoluted network activity. Bottom, unit spiking activity.

we normalized  $S$  by dividing all results by the largest recorded  $\max(S)$  over all simulations, thus placing all values in the range  $[0, 1.0]$ . We did this so that we could compare directly with the original Watts and Strogatz results of  $C$  clustering and  $L$  average path length, which we measured for our networks as well in order to reproduce the basic example of small-world network structure, and which were originally normalized in this same fashion. Also note that the figure use a  $\log_{10}$  scale for the  $p$  axis. This is done so that we can more easily see the phase transitions that occur in the measured network properties. Also note that this implies that much of the phase transition, especially for the  $L$  and our  $S$  measure, is occurring for fairly minimally wired networks, since  $p$  is somewhere in the range of  $0.01 \rightarrow 0.08$  or with only around 1% to 8% of connections being rewired. This shows that the introduction of a small number of long-range interconnections can have major effects. And that such networks can still be close to minimally wired, and thus have fairly low material resource requirements.

As shown in Figure 4, our network simulations do reproduce the phase

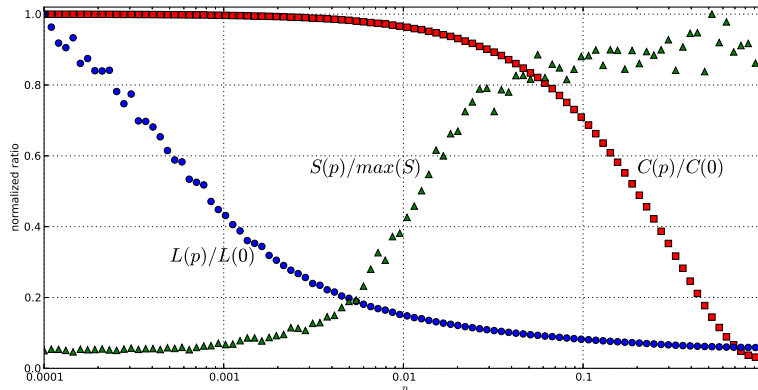


Figure 4: Simulation 1 results, comparison of  $S$  network synchronization activity measure, against  $C$  (average clustering) and  $L$  (average path length).

transitions of  $C$  and  $L$ . Network synchronization  $S$  (triangles) also shows a phase transition in the critical small-world region. For  $S$  the phase transition is happening between where  $L$  and  $C$  occur in the  $p$  space. So  $S$  does not begin to show much increase until  $L$  has mostly transitioned. However  $S$  has gone through most of its transition by the time  $C$  begins its phase change.

$S$  does not appear to be directly tied to the phase change of either  $C$  or  $L$  alone, but it is more directly related to and sensitive of changes in overall average path length. Also note that high  $S$  synchronization can be achieved only for fairly low  $L$ . But high global synchronization can be seen for networks either with high clustering  $C$  (around  $p = 0.02$ ) or low clustering ( $p$  from  $0.2 \rightarrow 1.0$ ). This brings up an interesting question: is global synchronization unaffected or unrelated to the clustering of units in the network? This observation motivates the question for the next simulation: what properties might be present that lessen the ability for networks to synchronize for larger  $p$ ?

### 3.2 Simulation 2: Effects of Propagation Delay on Synchronization

One obvious deficiency for studying global network synchronization is that the time to propagate signals is typically ignored. In many simulations of

network dynamics, there is no real notion of the spatial layout of units, nor the cost of wiring up such units in terms of material or delay of propagation of signals. In the second simulation, we added a propagation cost proportional to the wiring length of the connection carrying a spike signal. Distance is simply measured as the number of units around the ring (in shortest direction) one needs to go to get from the source to the destination of a spike signal. We added a buffer mechanism to the basic Izhikevich simulation, so that spike signals could be delivered to their destination with varying delays depending on their distance from source.

We found that networks with maximum delays of 20 were sufficient to demonstrate the effect, delay costs less than 10 usually began to show no effects on our simulations. For the simulations that follow, we used a distance scale of 25, meaning that units only 25 or less distance away on the ring experience a 0 propagation delay, while units from 26-50 distance away experienced a 1ms delay, up to 19ms propagation delay for units 451-500 distance on the ring. Therefore units have delays in propagating their spike firing inputs ranging from  $0 \rightarrow 19$ . This adds an additional burden on highly random networks, that have a large number of long range interconnections. In such networks, global activity is stifled by the time that it takes for signals to propagate over the long range connections. This, we believed, would have a similar effect to the propagation effects encountered by regular networks at the  $p = 0$  end of the space, that also experience propagation delays because of the need for multiple hops for information to propagate.

Figure 5 shows typical dynamics of networks in simulation 2. Propagation delays do not have much of an effect on regular networks nor networks with a small number of long range connections (we again show networks with  $p = 0, 0.02$  and  $1.0$  random rewiring). Long range connections in the small-world region, even with some delay, are still sufficient to help encourage global synchronization. However, the effects on high random  $p$  networks is a complete breakdown of coherent behavior (Figure 5, right). Here we can definitively see the effect that a lack of clustering cliquishness has on global network activity. With neither well organized neighborhood clusters, nor the ability to effectively and efficiently transfer information long distances, all coherent activity disappears from these networks.

As in simulation 1, we wanted to examine the overall synchronization  $S$  of networks with propagation delays. We again ran  $NUM\_SIMS = 100$  simulations for each  $p$  value reported. We reproduce all of the 3  $C$ ,  $L$  and  $S$  curves from the previous simulation, and impose the new  $S$  obtained on

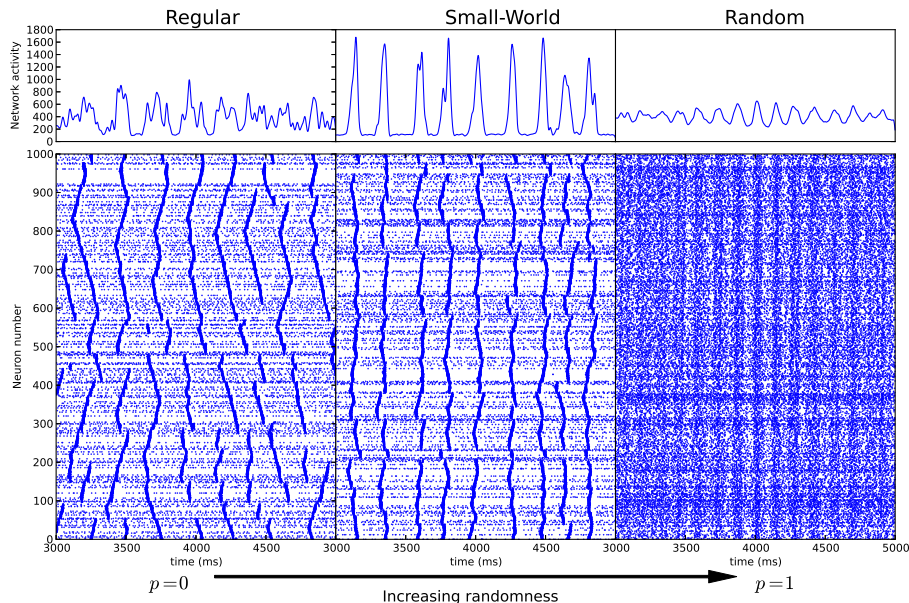


Figure 5: Example network dynamics of simulation 2. Left, regular lattice  $p = 0$ . Middle, small-world network  $p = 0.02$ . Right, random network  $p = 1$ . As before, the top part of figure depicts overall convolved network activity, while the bottom shows individual unit spiking activity.

networks with propagation delay. The results are shown in Figure 6.

With propagation delay in the network activity simulation,  $S$  still shows a phase transition in the small-world region, until a certain point (diamonds). At some point beyond  $p = 0.1$ , a combination of a lack of local cohesion from neighborhoods, coupled with insurmountable propagation delays in passing signals around the network, causes all coherent activity to cease. The breakdown of the delayed  $S$  synchronization performance appears to be related to the loss of clustering  $C$  of the networks. This makes sense, without delays we believe that the whole network in a sense forms a single large cohesive cluster, thus random networks are able to sustain global firing without small local neighborhood cluster. But with delays the loss of local neighborhood cluster to synchronize activity results in the loss of any overall coherent activity. This can be seen when comparing the dynamics in the simulation 2 random networks, to regular network dynamics, which while not globally synchronized, do display wavelets of coherent spike trains that propagate around the

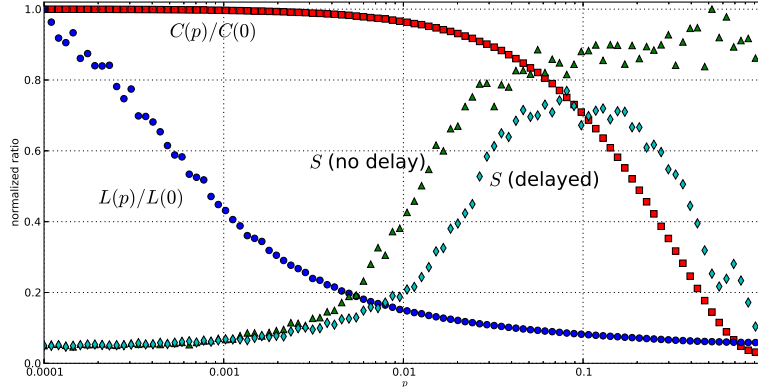


Figure 6: Simulation 2 results, comparison of  $S$  with no propagation delay (triangles) to  $S$  with propagation delay (diamonds).

ring spatially. This plot does show a limitation of our  $S$  measure, as there is a clear difference in activity from the  $p = 0$  end of the spectrum to the  $p = 1$  end of the spectrum (see previous Figure 5). At  $p = 0$  there is still group synchronization, but such waves are unable to organize into global patterns. While at  $p = 1$  There is no synchronization of any kind within the network, all activity is random firing of units.

## 4 Discussion

The presence of a phase transition of the global synchronization dynamics is a nice illustration that the effects a few long-range interconnections can have on global information transfer. In this research, we showed that spiking dynamics undergo such a phase transition with even a small number of long-range interconnections. But decreasing path lengths may not be the only factor in this transition. When other types of constraints are taken into account, for example the cost of propagating the signals over longer distances, we see that large numbers of long-range interconnections may be suboptimal in more than just material costs and constraints sense. The effect of transmission delays on global synchronization can only be overcome with networks in the small-world region, that balance just enough long range connections to allow for efficient global communication, but not so much that delayed



signals can't properly be correlated with one another by the network groups. Further, clustering may play a role in the ability of small-world networks to produce global synchronization. As long as local clustered groups are present when there are propagation delays, the network appears to be able to sustain coherent activity. With delays, if there are coherent groups then at least some coherent activity and information transfer is possible. But if there are no groups, randomness and incoherent activity will be the norm.

The presence of waves spreading out from a seed point, seen for regular networks and small-world networks that are sub-threshold for global synchronization, remind us a bit of Freeman's theory of collective synaptic synchronization, known as Freeman's theory of mass action [8, 7]. Freeman has demonstrated the presence of wavelets of activity in Brain EEG's, that seed from points in the neural tissue and spread outwards in synchronized mass action waves. These are different from regular synchronized oscillations, such as gamma and alpha waves. We speculate that the clustering of small-world networks can provide seed points for such wavelets of activity, and that sub-threshold synchronization allows for such seeds to propagate from group to group, rather than completely dominating global dynamics.

In this work we do assume global synchronization is an important property for information processing in dynamical spiking networks. This of course is not really true, too much synchronization is known to be a bad property, and can be signs of a seizure or other malfunction in the functional dynamics. It does appear that network dynamics need to be tuned towards organizations where they are close to, and able to sustain global waves of synchronization for short periods, but that mostly synchronize in more local groups. Small-world organization, with highly modular clustering, does appear to support this type of functional dynamic readily.

As we mentioned in the discussion of the experiment results,  $S$  is a crude measure of network synchronization. It certainly is incapable of detecting the wavelet patterns that high  $C$  neighborhoods seems to produce. In addition it is not able to determine if there are other frequency dynamics present in the networks, though of course we could always also examine the second, third, etc. dominant frequencies that are not harmonics of each other. Other measures of global organization, that don't depend on a local summed field potential, might be interesting to apply to these ring lattice organized networks. Perhaps measures of synchronized spiking activity based on a nodes friendship graph (immediate neighbor, 2nd neighbors, etc.) might be of interest. For the case where connections have a propagation delay, in effect a

distance weight (different from the action potential weight), we might want to examine groups based on the time of travel of signals on the shortest distance path between units.

In this research report we have concentrated solely on small-world network organization and its effects on spiking dynamics. Most complex real world networks, including brain networks, have properties that are not captured by the WS small-world interpolation. In particular, brain and other real networks show scale-free degree distributions, where the degree of a node is simply the count of the number of connections to or from the node [1]. For WS interpolated networks, degree distributions are fairly uniform at all points along the  $p$  spectrum. For scale-free degree distributions, there are present a few hub nodes that are highly connected, while the majority of nodes have very few connections. A similar analysis on the effects of interpolating between small-world networks with uniform degrees (WS small networks) to small-world networks with scale-free degree distributions would be an interesting follow up to this work. The presence of hub nodes in such networks provide short range paths, allowing for efficient global communication. However, clustering can be increased and decreased in such scale-free networks, to tune the amount of sub to critical threshold wavelet generation and global synchronization.

## 5 Conclusion

In the reported research, we showed the results of interpolating network structure from regular, through small-world regimes to random networks, on the functional dynamics of spiking networks. Functional dynamics of sparsely, but strongly connected spiking units depend critically on the network organization. Regular lattices are characterized by packets of spreading spike wavelets, that originate at a point and spread around the ring lattice. Without long-range connections, global synchronized behavior is not possible. At the other extreme, random networks are easily and strongly globally synchronized. Small-world networks begin to allow global organization rather quickly. Within the small-world region, larger groups become coherently connected with a few long-range connections, and global synchronized behavior emerges. We demonstrated that this emergence of global synchronization ( $S$ ) takes the form of a phase transition in the small-world region, similar to and between the phase transitions of clustering ( $C$ ) and average path length

(L).

In addition to exploring the functional dynamics of small-world networks, we looked at the effect of adding more realistic propagation delay constraints to the functional dynamics of such spatially constrained networks. Adding propagation effects of spike signals makes it impossible for random networks to sustain global synchronization behavior (once delays are sufficient). Only networks in the small-world region are able to successfully sustain global synchronized behavior when significant propagation delays are present. This is due to the presence of a small number of long-range paths that allow for information to be transmitted over the network globally, as well as the reinforcement of synchronized behavior through the tight coupling of neighborhood clusters. We showed that the phase transition in global synchronization breaks down under the presence of propagation delays, apparently as a function of the decreasing clustering in the network as they become more random.

## Acknowledgments

This work was partially supported by NSF grant #0916749 and DOE grant #DE-SC0001132. Simulation resources and time were provided by the Texas A&M - Commerce Lion HPC computing cluster.

## References

- [1] Réka Albert and Albert-László Barabási. Statistical mechanics of complex networks. *Reviews of Modern Physics*, 74(1):47–97, 2002, arXiv:cond-mat/0106096v1.
- [2] S. Boccaletti, V. Latora, Y. Moreno, M. Chavez, and D.-U. Hwang. Complex networks: structure and dynamics. *Physics Reports*, 424:175–308, 2006, doi:10.1016/j.physrep.2005.10.009.
- [3] Ed Bullmore and Olaf Sporns. Complex brain networks: graph theoretical analysis of structural and functional systems. *Nature Reviews Neuroscience*, 10:186–198, March 2009, doi:10.1038/nrn2575.
- [4] Zhidong Deng and Yi Zhang. Collective behavior of a small-world recurrent neural system with scale-free distribution. *IEEE*

- Transactions on Neural Networks*, 18(5):1364–1375, September 2007, doi:10.1109/TNN.2007.894082.
- [5] Andreas K. Engel and Wolf Singer. Temporal binding and the neural correlates of sensory awareness. *Trends in Cognitive Science*, 5(1):16–25, 2001.
  - [6] Paul Erdős and Alfréd Rényi. On the evolution of random graphs. *Publ. Math. Inst. Hungarian Academy of Sciences*, 5:17–61, 1960.
  - [7] Walter J. Freeman. *Mass Action in the Nervous System*. Academic Press, New York, 1975.
  - [8] Walter J. Freeman. A pseudo-equilibrium thermodynamic model of information processing in nonlinear brain dynamics. *Neural Networks*, 21(2-3):257–265, 2008.
  - [9] Eugene M. Izhikevich. Simple model of spiking neurons. *IEEE Transactions on Neural Networks*, 14(6):1569–1572, November 2003, doi:10.1109/TNN.2003.820440.
  - [10] Eugene M. Izhikevich. Which model to use for cortical spiking neurons. *IEEE Transactions on Neural Networks*, 15(5):1063–1070, September 2004, doi:10.1109/TNN.2004.832719.
  - [11] Stanley Milgram. The small world problem. *Psychology Today*, 1:63, 1967.
  - [12] Xiao Fan Wang and Guanrong Chen. Synchronization in small-world dynamical networks. *International Journal of Bifurcation and Chaos*, 12(1):187–192, 2002, doi:10.1142/S0218127402004292.
  - [13] L.M. Ward. Synchronous neural oscillations and cognitive processes. *Trends in Cognitive Science*, 7(12):553–559, 2003, doi:10.1016/j.tics.2003.10.012.
  - [14] D. J. Watts and S. H. Strogatz. Collective dynamics of small-world networks. *Nature*, 393:440–442, 1998, doi:10.1038/30918.